ISBN: 978-3-95450-168-7 doi:10.18429/JACoW-IPAC2015-TUPJE013

LATTICE DESIGN OF LOW BETA FUNCTION AT INTERACTION POINT FOR TTX-II*

Tenghui Rui, Wenhui Huang
Accelerator Laboratory, Department of Engineering Physics,
Tsinghua University, Beijing 100084, China

Abstract

TTX-II is a storage ring being designed at Accelerator Laboratory in Tsinghua University as the second phase of Tsinghua Thomson scattering x-ray source (TTX), to increase the average photon flux generated. To achieve a small beta function at the interaction point, four pairs of quadrupole magnets, whose focusing strengths are optimized, are added to the baseline. The lattice design is presented in this work.

INTRODUCTION

For a storage ring dedicated to the generation of X-ray by means of Thomson scattering, the transverse beam sizes at the interaction point have great influence on machine performance. The number of scattered photon in a collision between electron beam and laser beam is determined by the beam luminosity and total cross section of Thomson scattering [1].

$$n_\gamma = L\sigma \tag{1}$$

In laboratory frame, the luminosity is described by Eq. 2 [1].

$$L = \frac{n_e n_l / 2\pi}{\sqrt{\sigma_{ye}^2 + \sigma_{yl}^2}\sqrt{\sigma_{xe}^2 + \sigma_{xl}^2 + (\sigma_{se}^2 + \sigma_{sl}^2)\tan^2(\frac{\varphi}{2})}} \tag{2}$$

where $\sigma_{x,y,se}$ and $\sigma_{x,y,sl}$ denote the horizontal, vertical and longitudinal sizes of electron and laser beams at interaction point, $n_{e,l}$ the particle numbers of electrons and photons. The collision plane is horizontal and φ is the collision angle between electron and photon beams.

The transverse beam sizes at a specific location in a storage ring is determined by beam emittance and optical functions.

$$\sigma_{xe} = \sqrt{\epsilon_x \beta_x + \eta_x^2 \delta_p^2} \tag{3}$$

$$\sigma_{ye} = \sqrt{\epsilon_y \beta_y} \tag{4}$$

where ϵ_x and ϵ_y are the horizontal and vertical emittances, δ_p the momentum spread of the electron beam, η_x the dispersion function at IP, and β_x and β_y the horizontal and vertical beta functions at IP.

To reduce the transverse beam sizes at IP, either the betatron function or the emittance should be minimized. In this work, the design of a mini-beta lattice is presented.

* Work supported by National Natural Science Foundation of China(NSFC)(10735050,11127507).

MINI-BETA LATTICE

The baseline design of TTX-II and the previous mini-beta lattice design are discussed in [2, 3]. To avoid element intersection and to match the ring revolution frequency with synchronizing system frequency(2856 MHz), the ring circumference has to be changed. Moreover, the layout of the magnets has to be rearranged because the stripline kicker strength is not sufficient enough for beam injection. The layout of the current design is shown in Fig. 1.

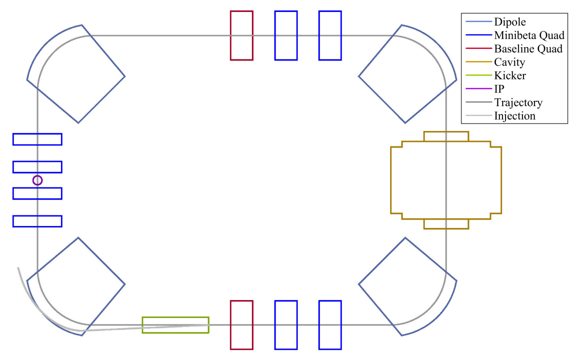

Figure 1: Layout of the mini-beta lattice.

Two pairs of quadrupoles are placed around the interaction point to provide strong focusing of the electron beam. Another two pairs of quadrupoles are placed in the straight sections between the baseline quadrupoles and bending magnets, to help adjust ring parameters such as working point and dispersion.

To find potential configurations for the lattice, all possible settings of quadrupole strengths are scanned and filtered by properties of interest such as betatron tunes and natural chromaticities. The time complexity of this algorithm depends exponentially on the number of variables, so the step size of scanning has to be large and we can only get a rough idea of what can be achieved with the current layout. For further optimization, genetic algorithm technique(GA) is exploited. To speed up convergence, the initial values of optimizing variables are chosen from the scan results. Then a population of possible settings are created and evolved by mimicking natural evolution process such as mutation, crossover and selection. The objective of GA is a function of lattice properties such as betatron tunes, beta functions and dispersion function at IP, natural chromaticities and momentum compaction factor. The program ELEGANT is used in the optimization process [4].

Figure 2 shows the optical functions of the optimized mini-beta lattice.

ISBN: 978-3-95450-168-7 doi:10.18429/JACoW-IPAC2015-TUPJE013

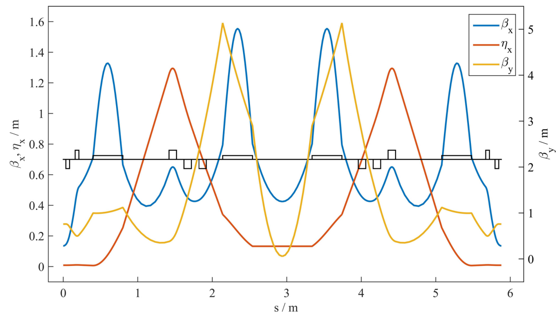

Figure 2: Optical functions of the mini-beta lattice.

Table. 1 summarizes the main parameters of the mini-beta lattice. The horizontal beta function is optimized to be 0.135m. The calculation of equilibrium beam parameters has taken into account the effects of intrabeam scattering(IBS), Thomson scattering and synchrotron radiation. The calculation of IBS induced emittance growth rate follows the Bjorken-Mtingwa formulation. Thomson scattering is approximated as wiggler radiation.

Table 1: Parameters of Mini-beta Lattice (* indicates IP)

Parameter	**Value**
Beta functions (β_x^* / β_y^*)	0.135 m / 0.775 m
Dispersion function (η_x^*)	8.77 mm
Betatron tunes (ν_x / ν_y)	1.72 / 1.39
Chromaticities (ξ_x / ξ_y)	-1.51 / -1.08
Momentum compaction factor (α_c)	0.175
Damping partition number (J_x)	0.947
Equilibrium Emittance (ϵ)	1.80 µm
Coupling Factor	0.1
Bunch Length(σ_L)	16.5 mm
Momentum Spread(δ_p)	0.119%
Beam Size(σ_x^* / σ_y^*)	0.493 mm / 0.373 mm
Beam Divergence($\sigma_{x'}^*$ / $\sigma_{y'}^*$)	3.65 mrad / 482 µrad

DYNAMIC APERTURE

Dynamic aperture is evaluated at IP by tracking simulation using the program ELEGANT. Figure 3 plots the dynamic aperture, including on-momentum and off-momentum particles. The tune shift with different momentum deviance is listed in Table 2. The dynamic aperture is approximately 30 times larger than the horizontal beam size at IP, so the dynamic aperture is sufficiently large enough.

To gain more insight about the particle diffusion process, frequency map analysis(FMA) is performed. Figure 4 shows the on-momentum particle dynamic aperture and its frequency map at interaction point with tune diffusion rate. The diffusion rate is indicated by color, whose definition is described by Eq. 5.The lower the diffusion rate, the more stable the particle. According to Fig. 4, the $2\nu_y - \nu_x = 1$ resonance line is the main cause of particle instability since the diffusion rate is high near it. Fortunately, the diffusion rate is small within $10\sigma_{x,y}$, so most particles would be stable.

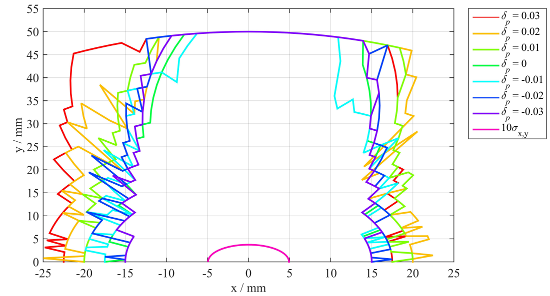

Figure 3: The dynamic aperture of the mini-beta lattice.

Table 2: Betatron Tunes with Different Momentum Deviations

δ_p	ν_x	ν_y
0.03	1.6814	1.3574
0.02	1.6929	1.3661
0.01	1.7057	1.3754
0	1.7200	1.3855
-0.01	1.7359	1.3967
-0.02	1.754	1.4094
-0.03	1.7745	1.4242

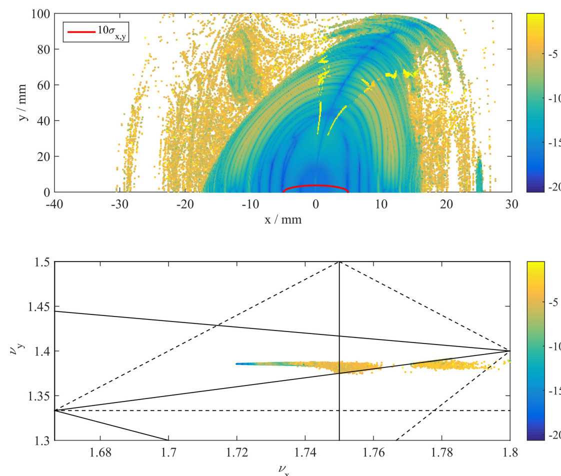

Figure 4: The dynamic aperture with diffusion rate of on-momentum particles.

$$d = \log_{10}(\Delta\nu_x^2 + \Delta\nu_y^2) \tag{5}$$

ERROR ANALYSIS

Manufacturing imperfection and excitation current errors introduce field strength errors. Field errors and misalignment errors together cause the closed orbit to deviate from the original designed trajectory. For a storage ring dedicated to electron-laser interaction, it's important to keep the trajec-

ISBN: 978-3-95450-168-7 doi:10.18429/JACoW-IPAC2015-TUPJE013

tory deviation at IP sufficiently small to ensure an optimal overlap between electron and laser beams. Moreover, these errors can cause tune shift and thus potential beam instability. Therefore, it's of great importance to determine whether these errors should be of concern and if so, how to correct them.

To calculate orbit distortion and tune shift, all possible errors are included in simulation with the assumption that the errors are independently and normally distributed. The main magnet errors are listed in Table. 3 [5]. The uncorrected orbit is illustrated in Fig. 5 and the RMS values are listed in Table. 4.

The closed orbit position displacements are over 5 times smaller than the beam sizes. However, the angle displacements seem large compared to beam divergence, but their absolute values are small. Therefore no significant impact on the number of Thomson scattered photons is expected. The shifted tunes due to errors are still in a safe region in the tune diagram, as can be seen in Fig. 6. In all, this lattice is tolerant enough to typical field and misalignment errors for electron-laser interaction.

Table 3: Main Magnet Errors

RMS Value	Dipoles	Quadrupoles
dB/B	10^{-4}	10^{-4}
dx, dy	0.2 mm	0.2 mm
Tilt	0.2 mrad	1 mrad
Edge Angle	1°	-

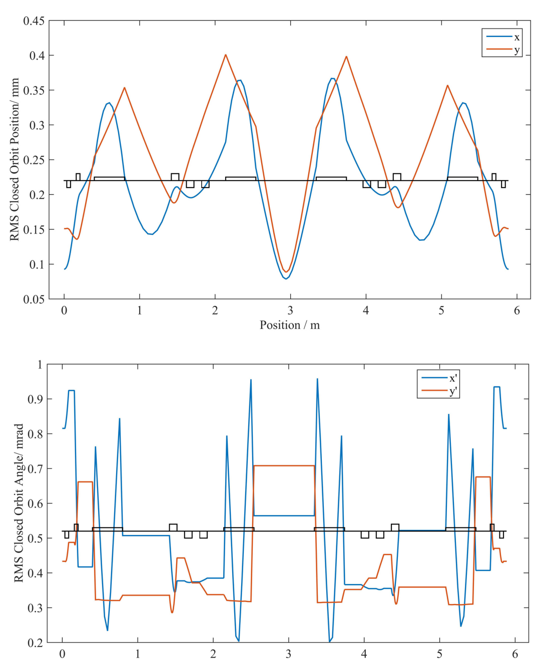

Figure 5: Uncorrected closed orbit.

Table 4: Closed Orbit Distortion

RMS Value	Max	IP
x	366.7 µm	92.9 µm
y	401.3 µm	151.1 µm
x'	959.1 µrad	815.4 µrad
y'	708.1 µrad	433.4 µrad

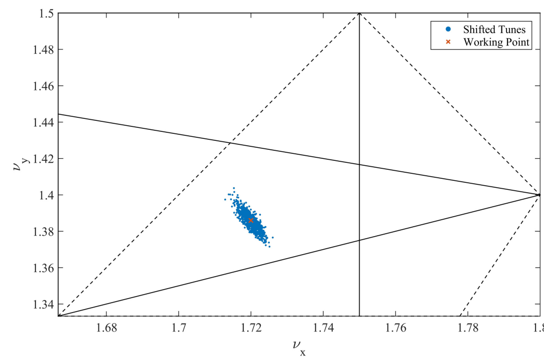

Figure 6: Tune spread due to field and misalignment errors.

CONCLUSION

The lattice design of low beta function at interaction point for Tsinghua Thomson scattering x-ray source is presented. Two pairs of quadrupoles are placed around the interaction point to provide strong focusing of the electron beam. Another two pairs of quadrupoles are placed in the straight sections between the baseline quadrupoles and bending magnets, to help adjust ring parameters such as working point and dispersion. The horizontal beta function is optimized to be 0.135m. The horizontal dynamic aperture is over 30 times larger than the horizontal beam size at IP, for momentum spread between -3% and 3%, and thus a long beam lifetime can be expected. Error analysis indicates that this lattice is tolerant to typical field and misalignment errors.

REFERENCES

[1] Wenhui Huang *et al.*, "Preliminary Study of X-Ray Source Based on Thomson Scattering", High Energy Physics and Nuclear Physics (Chinese Edition), 28 (4), April 2004, pp. 446-450.

[2] H.S. Xu *et al.*, "Design of a 4.8-m ring for inverse Compton scattering x-ray source", Physical Review Special Topics-Accelerators and Beams, 17.7 (2014) p. 070101.

[3] Tenghui Rui, Haisheng Xu, and Wenhui Huang, "Lattice Design of Low Beta Function at Interaction Point for TTX Compact Ring", in *Proc. SAP'14*, Lanzhou, China, Aug. 2014, paper WEPH27, p. 78.

[4] M. Borland, "Elegant: A flexible SDDS-compliant code for accelerator simulation", Advanced Photon Source, ANL, Argonne, IL, USA, Rep. LS-287.

[5] *ThomX Technical Design Report*, A. Variola, J. Haissinski, A. Loulergue, and F. Zomer, Eds., 2014, p. <in2p3-00971281>.